Detection and identification of antibacterial proteins in snake venoms using at-line nanofractionation coupled to LC-MS

Mladic, M.; Slagboom, J.; Kool, J.; Vonk, F.J.; Wezel, G.P. van; Richardson, M.K.

Toxicon 155 (2018) 66–74

Contents lists available at ScienceDirect

Toxicon

journal homepage: www.elsevier.com/locate/toxicon

Detection and identification of antibacterial proteins in snake venoms using at-line nanofractionation coupled to LC-MS

Marija Mladic[a], Julien Slagboom[a], Jeroen Kool[b], Freek J. Vonk[c], Gilles P. van Wezel[d], Michael K. Richardson[a,*]

[a] Animal Sciences and Health, Institute of Biology Leiden, University of Leiden, Sylviusweg 72, 2333BE, Leiden, The Netherlands
[b] Division of BioAnalytical Chemistry, Amsterdam Institute for Molecules Medicines and Systems, Vrije Universiteit Amsterdam, De Boelelaan 1083, 1081HV, Amsterdam, The Netherlands
[c] NCB Naturalis, Sylviusweg 72, 2333BE, Leiden, The Netherlands
[d] Molecular Biotechnology and Health, Institute of Biology Leiden, University of Leiden, Sylviusweg 72, 2333BE, Leiden, The Netherlands

ARTICLE INFO

Keywords:
Snake venom
Antibacterial activity
Liquid chromatography-mass spectrometry
Resazurin-reduction assay

ABSTRACT

This study describes the application of at-line nanofractionation to the screening of snake venoms for antibacterial activity against Gram-positive and Gram-negative bacteria, the detection of proteins of interest, and their partial or full identification. A method was developed to identify bioactive peptides in crude snake venoms based on reversed-phase liquid chromatography (LC), with parallel nanofractionation onto 384-well plates and mass spectrometry (MS). Bioactivity assays were based on a resazurin-reduction assay. Accurate masses of the bioactive peptides were determined, and peptides were then identified via nanoLC–MS/MS analysis of tryptic digests, allowing full or partial identification of the bioactive proteins. Crude venoms from 41 species were screened for their antibacterial bioactivity. Venoms showing the highest activity were further screened using at-line nanofractionation, which resulted in the elucidation of 28 bioactive proteins.

1. Introduction

The growing incidence of antibiotic resistance among pathogenic bacteria is becoming a serious threat to public health. Therefore, there is an urgent need for the discovery and development of new antibacterial compounds through traditional pipelines involving the isolation of natural products from microorganisms, and semi-synthetic and synthetic approaches. Moreover, new sources of antibacterial compounds are being explored, with special emphasis on the discovery and development of peptide antibiotics. Animal venoms, including those from snakes, represent a potential alternative source of peptide antibiotics. Snake venoms are produced in a modified salivary gland and represent a cocktail of compounds, mainly peptides and proteins, evolved to efficiently immobilize the prey organism. Many academic groups have put significant efforts into studying snake venoms and understanding their biological effects. Moreover, snake venoms have traditionally served as an important source of compounds in drug discovery (Cook et al., 1999; King, 2011; Ryan J. R. McCleary, 2015; Scarborough, 1999; Smith and Vane, 2003).

On the antibacterial properties of both crude snake venoms and compounds purified from snake venoms, many studies have been conducted. The antibacterial activity of snake venoms is mostly attributed to enzymes, such as phospholipases A2 (PLA_2s), snake venom metalloproteinases (SV-MPs) and snake venom L-amino acid oxidases (SV-LAAOs) (de Oliveira Junior et al., 2013), which are all proteins with molecular masses in the range of 13–60 kDa in a monomeric form. Some studies reported the identification of antibacterial peptides in snake venoms such as cathelicidins (Wang et al., 2008), crotamine (Oguiura et al., 2011) and peptides from the waprin family, nawaprin (Torres et al., 2003) and omwaprin (Nair et al., 2007). Moreover, peptides have been synthesized based on these proteins and studied for their antibacterial activity (Okubo et al., 2012; Paramo et al., 1998; Santamaria et al., 2005). For detailed reviews on this subject, the reader is referred elsewhere (de Oliveira Junior et al., 2013; Munoz, 2014).

The detection of bioactive proteins in snake venoms and their identification are typically done using bioassay-guided fractionation (BGF). This means that the constituents of crude venom are first fractionated, commonly by using size-exclusion chromatography (SEC). The post-column collected fractions are then exposed to a bioassay. For application to the discovery of antibacterial compounds, the fractions

* Corresponding author.
E-mail addresses: m.mladic@biology.leidenuniv.nl (M. Mladic), julien_slagboom@hotmail.com (J. Slagboom), j.kool@vu.nl (J. Kool), research.vonk@naturalis.nl (F.J. Vonk), g.wezel@biology.leidenuniv.nl (G.P. van Wezel), m.k.richardson@biology.leidenuniv.nl (M.K. Richardson).

https://doi.org/10.1016/j.toxicon.2018.08.009
Received 24 April 2018; Received in revised form 20 August 2018; Accepted 27 August 2018
Available online 31 August 2018
0041-0101/

collected are tested for their antibacterial activity against bacterial strains of interest, often by using the agar diffusion assay (Wang et al., 2008). Fractions containing the highest bioactivity are then subjected to a second round of liquid chromatography (LC) separation, fractionation, and bioassaying. Depending on the size and nature of bioactive compounds, the second separation is performed using ion-exchange chromatography (IEC) or reversed-phase liquid chromatography (RPLC), and in some cases both separations are performed. The purity and mass of the compounds are checked at this stage using mass spectrometry (MS) and sodium dodecyl sulfate-polyacrylamide gel electrophoresis (SDS-PAGE). After this, the sequence of the peptide/protein is determined using MS or Edman degradation.

Bioassay-guided fractionation led to the successful isolation and identification of many bioactive compounds from snake venoms, among which are the ones with antibacterial activity. Examples are the peptide vgf-1 from venom of the Chinese cobra *Naja atra*, active against multidrug resistant *Mycobacterium tuberculosis* (Xie et al., 2003), and the peptide microporin from the venom of the scorpion *Isometrus maculates*, effective against multiple antibiotic resistant bacteria (Zhao et al., 2009). However, it should be noted that the workflow applied in this approach can be time-consuming, mostly because the bioassays and chemical identification are conducted separately. For this reason, methods in which the bioassays are coupled directly in parallel to chemical characterization were introduced. The first of these methods is based on so-called high-resolution screening in which LC effluent is split post-column; one half of the flow goes to MS while the other half is mixed on-line with bioassay reagents followed by continuous flow incubation and detection of the (often fluorescence) bioassay response, which is recorded in time as a bioactivity chromatogram (Heus et al., 2013; Otvos et al., 2013). The bioactive peaks detected in the bioassay are aligned to their *m/z*-values, detected in the LC-MS measurement, based on the peak shape and retention time. In this way the bioactivity readout and chemical characterization are performed in parallel, shortening the time needed to identify the bioactive compounds. The drawback of this approach is that it can be used only for bioassays that have short incubation times. Most recently, this issue was tackled by applying methods based on a so-called at-line nanofractionation approach (Mladic et al., 2016). This newly introduced approach relies on the concept of BGF and represents off-line coupling of the bioassay to the LC–MS analysis using high-resolution post-column fractionation (i.e. nanofractionation) as the linking technology.

At-line nanofractionation methods were developed for the detection and identification of the bioactive compounds that affect the activity of various enzymes, such as thrombin, factor Xa and angiotensin-converting enzyme (Mladic et al., 2016, 2017). In this approach, LC separation of crude venoms is followed by a post-column flow split, which enables parallel MS detection and high-resolution (e.g. 6 s/well) nanofractionation onto 384-well plates. To eliminate the influence of organic modifiers present in the mobile phase, the nanofractions collected are subjected to evaporation in a speed-vac centrifuge and the bioassay reagents are then pipetted into the wells containing dried nanofractions. The bioassay readout of each well is plotted against the time when the nanofraction was collected resulting in a reconstructed bioactivity chromatogram in which the bioactive compounds are displayed as peaks with either positive or negative maxima. The *m/z*-values of the bioactive peaks are determined from the parallel MS measurements by plotting the extracted ion currents (XICs) of all the *m/z*-values present in the MS spectrum at the time when the bioactivity elutes. The correlation of the bioactive peaks and XICs is based on peak shape and retention time (Mladic et al., 2016).

In this study, we have used an optical density microtiter plate assay to evaluate antibacterial activity in venoms from 41 different species of snake against strains of *Bacillus subtilis* and *Escherichia coli*. At-line nanofractionation was used to screen venoms from 14 species, based on initial antibacterial properties. After reconstruction of the bioactivity chromatograms, the *m/z*-values of the bioactive peaks detected were determined. The bioactive peptides were then determined using nanoLC–MS/MS analysis of tryptic digests of the bioactive peptides.

2. Materials and methods

2.1. Chemicals and stock solutions

All solvents used in this study were analytical grade. Acetonitrile (ACN) and formic acid (FA) were purchased from Biosolve (Valkenswaard, The Netherlands) and water was purified using a Milli-Q plus system (Millipore, Amsterdam, The Netherlands). Glycerol, ethanol, β-mercaptoethanol, iodoacetamide, NH_4HCO_3, NaCl, yeast extract, tryptone, agar, amoxicillin and chloramphenicol were obtained from Sigma-Aldrich (Zwijndrecht, The Netherlands). Kanamycine and nalidixic acid were obtained from Duchefa Biochemie B.V. (Haarlem, The Netherlands). The antibiotics were stored at −20 °C as stock solutions. Amoxicillin (100 mg/mL), kanamycine (50 mg/mL) and nalidixic acid (50 mg/mL) were diluted in water, while chloramphenicol (25 mg/mL) was diluted in ethanol. OP-145 was kindly given by Prof. Drijfhout and Prof. Nibbering (LUMC, Leiden, The Netherlands). Sequencing-grade modified trypsin was purchased from Promega Benelux B.V. (Leiden, The Netherlands), and stored and handled according to the manufacturer's instructions. Resazurin sodium salt was obtained from Brunschwig Biochemie B.V. (Amsterdam, The Netherlands) and stored at −20 °C as an aseptically prepared 15-mg/mL stock solution in water. All the snake venoms used in this study were obtained from Serpo (Rijswijk, The Netherlands) and stored in lyophilized form at −20 °C. Prior to analysis, the crude snake venoms were diluted in water under aseptic conditions to give a 5-mg/mL final concentration. After the analysis, the stock solutions were stored at −80 °C for later use.

2.2. Liquid chromatography, at-line nanofractionation and mass spectrometry

Liquid chromatography separation, subsequent at-line nanofractionation and parallel mass spectrometry analysis were performed in an automated fashion. For the LC separation, a Shimadzu UPLC system ('s Hertogenbosch, The Netherlands) was used. All the settings of the system were controlled via the Shimadzu Lab Solutions software. A Shimadzu SIL-30AC autosampler was set on a 50-µL injection. The two Shimadzu LC-30AD pumps were set on a total flow rate of 700 µl/min. A binary gradient was delivered to a 100 × 4.6 mm Waters Xbridge Peptide BEH300 C18 analytical column with a 5-µm particle size and a 300 Å pore size, which was guarded using a 3.9 × 5 mm Waters Xbridge BEH C18 guard column with a 5-µm particle size and a 130 Å pore size. The separation was carried out at 30 °C in a Shimadzu CTD-30A column oven. Mobile phase A was composed of 98% H_2O, 2% ACN and 0.1% FA, and mobile phase B was composed of 98% ACN, 2% H_2O and 0.1% FA. A linear increase of mobile phase B from 0% to 50% in 20 min was followed by a linear increase from 50% to 90% B in 4 min and a 5-min isocratic elution at 90% B.

Next, the initial separation conditions were reached in 1 min and the column was equilibrated at 0% B for 10 min. After the column, the flow was split in a 1:9 ratio. The smaller fraction was sent to the Shimadzu SPD-M30A photodiode array detector followed by a MaXis impact quadrupole–time-of-flight (qTOF) mass spectrometer (Bruker, Bremen, Germany). The larger fraction was sent to a nanofraction collector, a modified Gilson 235P autosampler. The mass spectrometer was equipped with an electrospray ionization source (ESI) and operated in positive-ion mode. The parameters of the ESI source were: source temperature 180 °C, capillary voltage 4.5 kV, dry gas flow 4 L/min and nebulizer at 0.4 bar. Full MS spectra were recorded in an *m/z* 50–3000 range at 1 spectrum/s rate. Bruker Compass software was used for the instrument control and data analysis. The nanofractions were collected in a serpentine fashion using Ariadne, in-house written software,

allowing for 6-s nanofractions to be collected onto the black 384-well plates (Greiner Bio One, Alphen aan den Rijn, The Netherlands) with maximum of four plates in a row. Each chromatographic run was collected onto 300 wells of the 384-well plate. After the nanofractionation, the plates were dried for approximately 18 h using a Christ Rotational Vacuum Concentrator (Salm en Kipp, Breukelen, The Netherlands) RVC 2-33 CD plus. The dried plates were then stored at −20 °C until the bioassay or tryptic digestion was performed.

2.3. Bacterial cell culture

Bacterial strains in this study were *Bacillus subtilis*, the antibiotic-sensitive strain *Escherichia coli* AS19 (Sekiguchi and Iida, 1967) and *E. coli* ET8. The latter is a derivative of *E. coli* ET12567 that carries a number of additional resistance genes, and is therefore resistant to beta-lactam antibiotics, streptomycin, tetracycline, chloramphenicol, neomycin, kanamycin and apramycin (Zhu et al., 2014). The cells were cultured in the in-house prepared LB agar and LB broth at 37 °C. Chloramphenicol and kanamycin were added to the growth medium of *E. coli* ET8 cultures as selection markers in final concentrations of 25 and 50 μg/mL, respectively.

2.4. Bacterial strains and antibacterial activity assessment

The antibacterial activity of crude snake venoms was tested in the Bioscreen C (Labsystems, Helsinki, Finland) automated growth curve analysis system, which is a plate reader that reads the light absorbance in the honeycomb microtiter plate with 100 wells. For this, bacterial overnight cultures were grown in the LB broth to a density of O.D. 0.2–0.5 measured at 600 nm. The cells were then diluted in LB to the final O.D. 0.01. To remove the added antibiotics, the *E. coli* ET8 cells were washed 2 times prior to dilution by centrifuging the cells at 6000 rpm for 2 min using Centrifuge 5415 C (Eppendorf, Nijmegen, The Netherlands) and re-suspending them in the fresh LB broth (no antibiotics added). Diluted cells were then added to the wells of honeycomb plates, which contained 5 μL crude snake venom (5 mg/mL) and appropriate controls. The final volume in the plates was 100 μL. The growth of the bacteria was measured for 18 h using the following settings on the Bioscreen C: wideband O.D. measurement, 30-min frequency of the measurements, 37 °C incubation temperature, 45 min preheating time, and continuous shaking at medium speed. Research Express software was used for the instrument control and data acquisition. The data obtained in the Excel sheet were transferred to GraphPad Prism 7 software (La Jolla, CA, USA) to plot the growth curves.

2.5. Resazurin reduction assay for antibacterial activity assessment

The antibacterial activity of the nanofractionated snake venoms was tested in the resazurin reduction assay. Bacterial overnight cultures were grown in the LB broth to a density of O.D. 0.2–0.5 measured at 600 nm. The cells were then diluted in LB to the final O.D. 0.0025. To remove the added antibiotics, the *E. coli* ET8 cells were washed 2 times prior to dilution by centrifuging the cells at 6000 rpm for 2 min using Centrifuge 5415 C (Eppendorf, Nijmegen, The Netherlands), and re-suspending them in the fresh LB broth (no antibiotics added). Resazurin solution was then added to the cells to a final concentration of 15 μg/mL and 25 μL/well of this mixture was directly pipetted onto 384-well plates containing dried nanofractions. Directly after this, the plates were centrifuged for 10 s at 1500 rpm using Centrifuge 5810 (Eppendorf, Nijmegen, The Netherlands) and subsequently incubated without the lids in a humidified incubator at 37 °C. The duration of incubation was 2 h for *B. subtilis* and 4 h for *E. coli* ET8. After the incubation, the fluorescence in the wells was measured as a single point measurement using a Victor3 Plate Reader (PerkinElmer, Inc, Waltham, MA, USA) at 550 nm excitation and 590 nm emission wavelengths. The fluorescent readout was normalized by dividing each value measured with the median of all the values obtained in a single measurement. Subsequently, the bioactivity chromatograms were plotted in a graph showing the normalized response of each nanofraction versus time at which each nanofraction was collected. Microsoft Excel 2010 (Redmond, Washington, USA) and GraphPad Prism 7 software (La Jolla, CA, USA) were used for the bioassay data analysis.

2.6. Tryptic digestion

The tryptic digestion was performed directly on the content of bioactive wells. After the bioactive wells were identified, 40 μL of water was added to these wells and incubated for 30 min at room temperature to allow dissolving of the proteins present in the wells. Next, 10 μL of the protein solution was transferred to an Eppendorf tube containing 15 μl of digestion buffer (25 mM NH_4HCO_3, pH 8.2). Subsequently, 1.5 μl of reducing agent (0.5% β-mercaptoethanol) was added to the tube followed by 5-min incubation at 95 °C. After incubation, the samples were cooled down to room temperature and 3 μL of alkylating agent (55 mM iodoacetamide) was added to the tube followed by 20-min incubation at room temperature in the dark. Finally, 1 μL of 0.1 μg/μL trypsin was added to the tube and incubated at 37 °C. After 1.5 h, an additional 1 μl of trypsin was added to the tube and the incubation was continued overnight. The samples were centrifuged the following day for 10 s at maximum speed in the Centrifuge 5424 (Eppendorf, Nijmegen, The Netherlands) and the supernatants were transferred to new tubes. Subsequently, the digestion was stopped by adding 1 μL of 5% FA to the tubes. The samples were then transferred to autosampler vials and analyzed using nanoLC-MS/MS.

2.7. nanoLC-MS/MS of tryptic digests and data analysis

For the analysis of tryptic digests an UltiMate 3000 RSLCnano system (Thermo Fisher Scientific, Ermelo, The Netherlands) was used followed by the MaXis impact qTOF mass spectrometer. The autosampler was run in partial-loop injection mode using 1-μL injection volume. Separation was performed on an analytical capillary column (150 mm × 75 μm) packed in-house with Aqua C18 particles (3 μm particle size and 200 Å pore diameter; Phenomenex, Utrecht, The Netherlands). The mobile phases consisted of eluent A (98% H_2O, 2% ACN, 0.1% FA) and eluent B (98% ACN, 2% H_2O, 0.1% FA). The following gradient program was used for separation: 2-min isocratic separation at 5% B, linear increase to 80% B in 15 min, 3-min isocratic elution at 80% B, decrease to 5% B in 0.5 min and equilibration for 9 min. The column was kept at 30 °C in the column compartment. Detection was carried out by a Variable Wavelength Detector set at 254 nm followed by a Bruker MaXis q−TOF mass spectrometer (Bruker, Bremen, Germany). The mass spectrometer had an electrospray ionization (ESI) source and was operated in positive-ion mode. Typical settings of the ESI source parameters for the MS instrument were the following: source temperature 200 °C, capillary voltage 4.5 kV and gas flow 10 L/min. Spectra were acquired at 1 spectrum/s in the range of m/z 50 to 3000. MS/MS spectra were recorded in data-dependent mode using 35-eV collision energy in the CID collision cell. Bruker Compass software was used for the instrument control and data analysis.

Protein identification was performed using MASCOT (Matrix Science, London, United Kingdom) search against Swiss-Prot and NCBInr 20150203 databases. The following parameters were specified: ESI-QUAD-TOF as the instrument type, trypsin as the digestion enzyme allowing for one missed cleavage, carbamidomethyl on cysteine as a fixed modification, oxidation on methionine as a variable modification, ± 0.2 Da peptide mass tolerance, and ± 0.05 Da fragment mass tolerance.

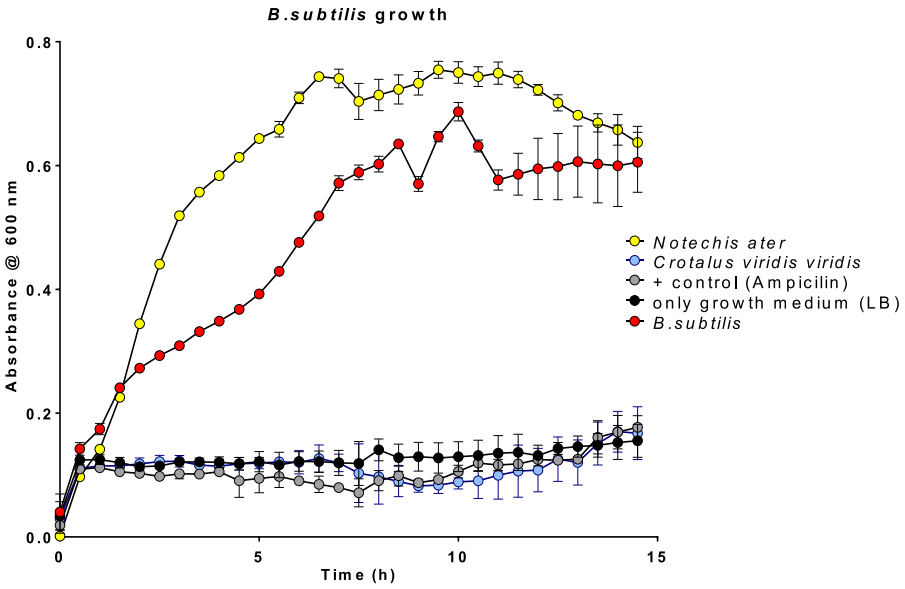

Fig. 1. Bacterial growth curves obtained from the screening of crude snake venoms for growth inhibition of *Bacillus subtilis*. The experiment was performed in a 100-well honeycomb plate with a 100-µL end-volume. The bacterial growth was measured in 30 min intervals over a 15 h period and expressed as the absorbance at 600 nm. Each data point represents the mean absorbance ± SD of triplicate wells. The normal growth of *B. subtilis* is shown with red circles (negative control) and the absence of bacterial growth in the wells containing only growth medium is shown with black circles. In the presence of ampicillin (4 µg/well), the bacterial growth was fully inhibited (gray circles), while in the presence of a crude snake venom (10 µg/well) bacterial growth was inhibited by *Crotalus viridis viridis* crude venom (blue circles) and not by *Notechis ater* crude venom (yellow circles). (For interpretation of the references to colour in this figure legend, the reader is referred to the Web version of this article.)

3. Results

3.1. Antibacterial activity of crude venoms

As a first step crude snake venoms were screened for antibacterial activity. Snake venoms (25 µg/well) and controls were added to the honeycomb wells in triplicate. As a positive control an antibiotic was added to the wells (5 µg/well of nalidixic acid for *E. coli* AS19 and *E. coli* ET8, and 4 µg/well of ampicillin for *B. subtilis*), while the wells containing only bacterial cells were used as a negative control. In addition, 3 wells containing growth medium only were used as a control of the bacterial growth and eventual cross-well contamination. The bacterial growth was measured as absorbance at 600 nm.

A typical example of the results obtained after the crude venom screening against *B. subtilis* is shown in Fig. 1. As expected, no bacterial growth was observed in the wells containing only growth medium or ampicillin, while the wells containing bacteria did show growth. Fig. 1 further shows examples of a snake venom with no antibacterial activity (*Notechis ater*) and a snake venom with high antibacterial activity (*Crotalus viridis viridis*).

In total, venoms from 41 snake species were screened against three different bacterial strains. Thirty-one venoms showed activity against at least one of the strains tested. The results of this screening are summarized in Fig. 2 as the semi-quantitative measure of the antibacterial activity of each venom. Fig. 2 further shows the antibacterial activity mapped onto a phylogenetic tree. All the viperid species tested showed relative high antibacterial activity, while antibacterial activity of elapid species varied between the species. All results of the initial crude venom screening against the three bacterial strains are presented as bacterial growth curves in Supporting Information Figs. S1–S6.

3.2. Antibacterial activity of snake venoms after at-line nanofractionation, detection and identification of antibacterials

Snake venoms that showed high antibacterial activity were screened for the presence of antibacterial compounds using at-line nanofractionation. After LC solvent evaporation, the antibacterial activity of the nanofractions collected was assessed in a resazurin reduction assay. This assay is based on the ability of viable bacterial cells with active metabolism to reduce the non-fluorescent resazurin substrate into a fluorescent resorufin product. Thus, if the mixture of cells and resazurin is added to the wells containing nanofractions without antibacterial compounds, a certain level of fluorescence representing the basal signal will be reached after incubation. In the presence of an antibacterial compound in a nanofraction, this basal fluorescence signal will be reduced and as consequence be manifested in the bioactivity chromatogram as a peak with a negative maximum.

In hyphenation of LC−MS analysis to the bioassay, advantages of using the resazurin reduction assay over the honeycomb plate assay are the following: 1) the resazurin reduction assay is performed in standard black 384-well plates whose dimensions are compatible with all the equipment used including the nanofractionation collector, plate reader, multichannel pipettes and automatic liquid handling devices; 2) the readout of the assay is fluorescence, which is sufficiently specific and sensitive to quantify small amounts of bioactive compounds; and 3) the readout of the assay is a rapid single point measurement, which makes it more high-throughput.

Results of the resazurin reduction assay were plotted into the bioactivity chromatograms that were then aligned to the corresponding LC−MS chromatograms. The alignment was done on the basis of the elution time of the peaks. Since the LC effluent was split post-column in a different ratio, the fraction arriving at the MS had a certain delay compared to the fraction that was delivered to the nanofractionation device. After the delay was determined and alignment of the chromatograms corrected accordingly, the monoisotopic masses measured in the MS were assigned to the bioactive peaks detected in the bioactive chromatograms. This was done in four steps. Firstly, the time point of the negative peak maximum was determined for each peak in the bioactivity chromatogram and assigned to the respective time point in the total ion current (TIC) of the corresponding LC−MS chromatogram. Secondly, an MS spectrum for each bioactive was plotted by averaging the spectra taken around the time of the peak maximum and subtracting the background spectra. Next, the extracted ion currents (XICs) of all masses detected in the MS spectrum were plotted and assigned to the corresponding activity peaks based on retention time and peak shape. Finally, the accurate monoisotopic masses were assigned to the bioactivity peaks using the deconvolution option in the MS software. Lastly, the contents of the bioactive wells from a replicate plate were subjected to tryptic digestion in order to identify the bioactive proteins.

In order to determine the delay between the MS and the bioassay, we first fractionated different concentrations of the positive control OP-145, a synthetic antibacterial peptide developed from a screen of human cathelicidin LL-37. The plates containing nanofractionated OP-145 were tested for antibacterial activity against *B. subtilis*, results of which are shown in Fig. 3 for the three injected concentrations tested (i.e. 3000, 300 and 30 µg/ml). As expected, the assay showed the

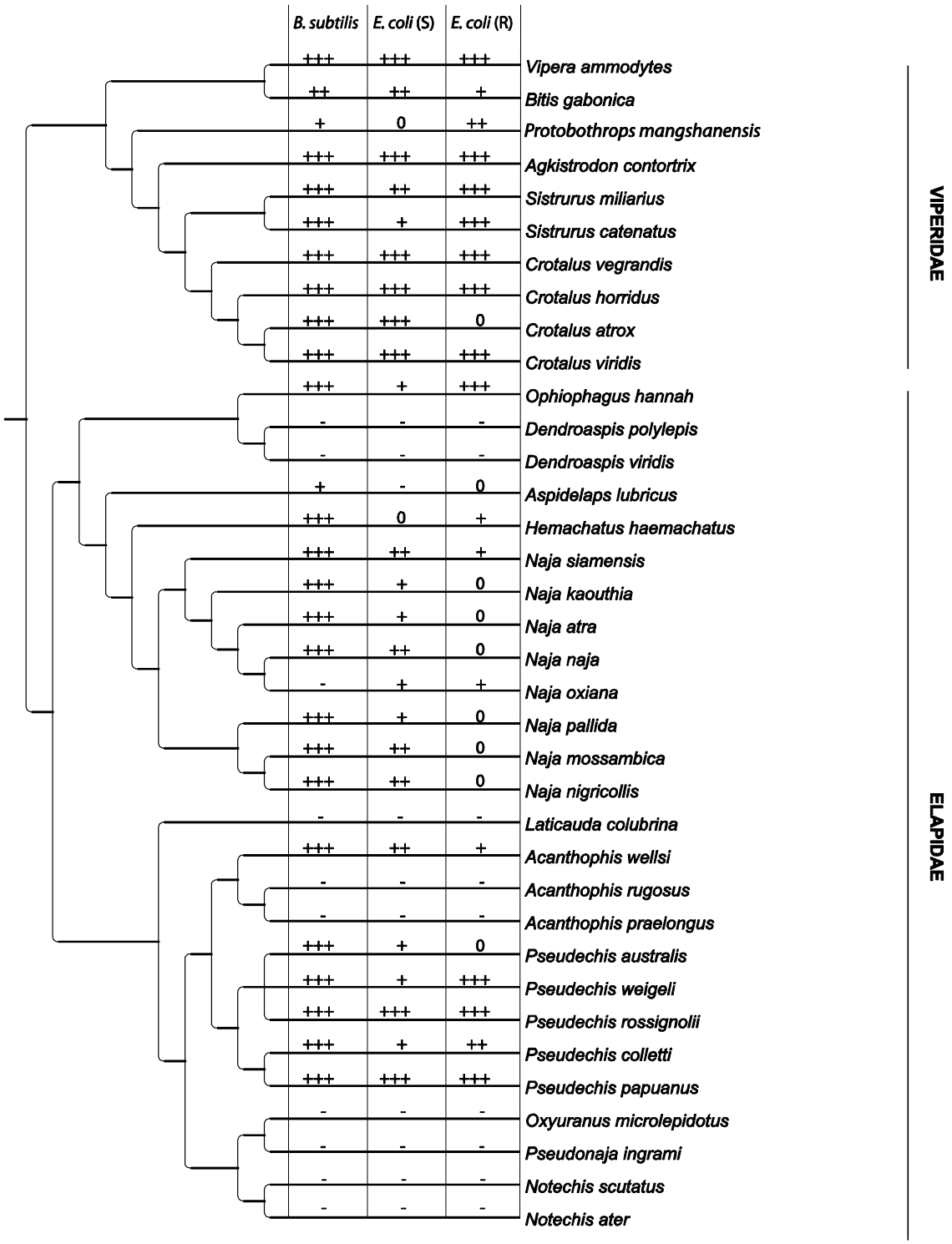

Fig. 2. Phylogenetic tree of the snake species used for testing of antibacterial activity of crude snake venoms. The tree shows the phylogenetic connections between the species tested and the semi-quantitative results of the antibacterial activity. Bioactivity of crude venoms: – no activity, 0 very low activity, + low activity, + + moderate activity, + + + high activity.

concentration-dependent response as the bioactivity peaks of OP-145 in the bioactivity chromatograms become narrower with injection of lower concentrations.

Next, 14 crude venoms were selected on the basis of their antibacterial properties and screened using the at-line nanofractionation approach from which in total 28 bioactive proteins were detected. The results of the screening are summarized in Table 1.

For proof-of-principle for detection and identification of the bioactive peaks after at-line nanofractionation, venom from *C. viridis viridis* was spiked with OP-145 (final concentration 30 µg/mL corresponding to the total amount of 1.5 µg at 50- µL injection) and screened for antibacterial activity against *B. subtilis* (Fig. 4). In total, three bioactive peaks were detected in the bioactivity chromatogram (Fig. 4, *i*). The following *m/z*-values were assigned to the bioactive peaks: *m/z*

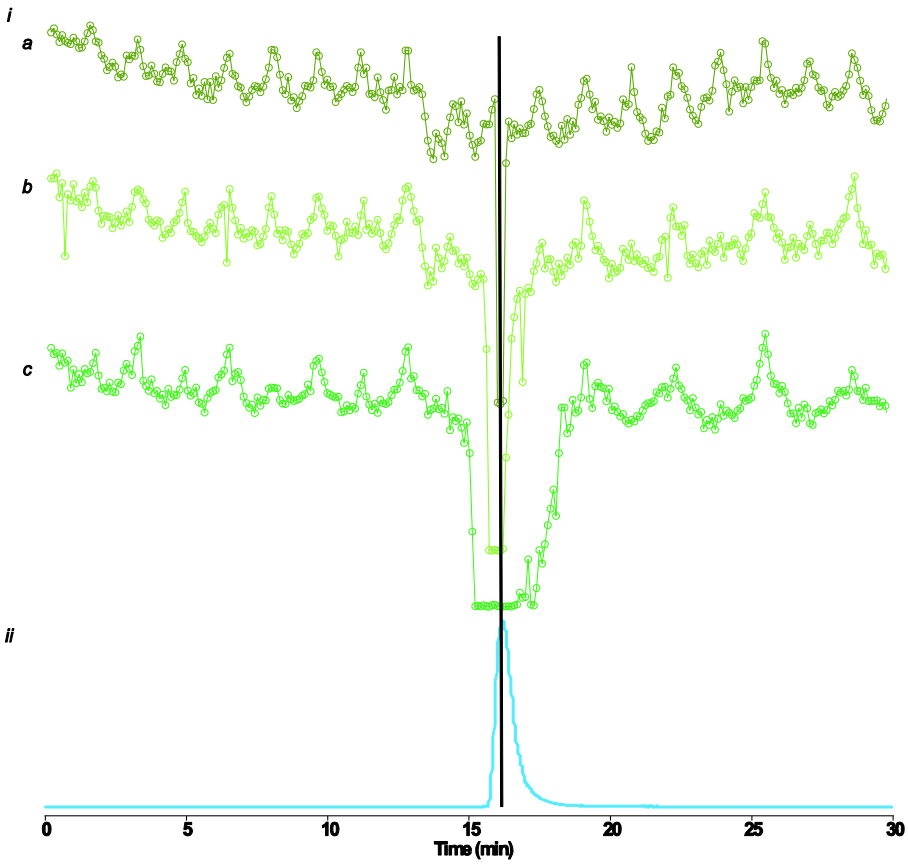

Fig. 3. Antibacterial activity of the positive control OP-145 against *Bacillus subtilis* after at-line nanofractionation. *a-c* Bioactivity chromatograms represent the results of the resazurin reduction assay for each nanofraction plotted against the time the nanofraction was collected. The peaks with negative maxima represent OP-145 injected at different concentrations 30 µg/mL (*a*), 300 µg/mL (*b*) and 3000 µg/mL (*c*). The bottom chromatogram represents the extracted ion current (XIC) of OP-145.

1378.8572^{10+}, 750.6825^{6+}, 1419.0639^{10+}, and 516.4200^{6+}, corresponding to the monoisotopic masses: 13769.4645, 4496.0465, 14203.5345, and 3091.9036 Da. The third peak was immediately assigned to OP-145 based on the retention time and the molecular mass detected.

Based on the XICs found to correspond to the bioactive peaks, it is

Table 1
List of the bioactive compounds found after at-line nanofractionation of crude snake venoms.

N° bioactive compound	Organism	Accurate *m/z* values	Deconvoluted monoisotopic mass (Da)	Calculated monoisotopic mass (Da)	(Predicted) toxin class
1	*Sistrurus catenatus tergeminus*	n.a.	n.a.	13729.1639	PLA_2
2	*Naja nigricollis*	1477.3307^{9+}	n.a.	13278.8804	PLA_2
3	*Naja nigricollis*	971.1988^{7+}	6787.3314	6787.3355	3FTx
4	*Naja nigricollis*	959.3384^{7+}	n.a.	n.a.	3FTx
5	*Naja nigricollis*	984.782^{7+}	6882.4112	n.a.	3FTx
6	*Naja nigricollis*	974.9141^{7+}	6813.3339	6813.3334	3FTx
7	*Crotalus vegrandis*		14175.4192	n.a.	PLA_2
8	*Naja kaouthia*	998.9422^{7+}	Approx. 6981.404	n.a.	3FTx
9	*Naja kaouthia*	980.6412^{7+}	6852.4216	n.a.	3FTx
10	*Naja naja*	963.6339^{7+}	6734.3761		3FTx
11	*Naja mossambica*	1477.3292^{9+}	13277.8880	13277.8962	PLA_2
12	*Naja mossambica*	971.1993^{7+}	6788.2602	6787.3355	3FTx
13	*Naja mossambica*	959.3389^{7+}	6705.2371	n.a.	3FTx
14	*Naja mossambica*	984.7818^{7+}	6883.3309	n.a.	3FTx
15	*Naja mossambica*	975.0555^{7+}	6815.2409	6813.3334	3FTx
16	*Pseudechis rossignolii*	1444.5596^{9+}	12982.9446	12982.9222	PLA_2
17	*Pseudechis rossignolii*	1448.5485^{9+}	13018.8424	13019.8144	PLA_2
18	*Hemachatus haemachatus*	971.2156^{7+}	6787.3749	6787.4472	3FTx
19	*Hemachatus haemachatus*	977.5035^{7+}	6831.4611	6831.4556	3FTx
20	*Hemachatus haemachatus*	987.2098^{7+}	6898.4080	6903.4177	3FTx
21	*Hemachatus haemachatus*	986.3406^{7+}	6892.3215	n.a.	3FTx
22	*Hemachatus haemachatus*	969.9176^{7+}	6778.3583	n.a.	3FTx
23	*Hemachatus haemachatus*	984.0551^{7+}	6876.3210	n.a.	3FTx
24	*Pseudechis colletti*	1457.9859^{9+}	13103.7847	n.a.	PLA_2
25	*Pseudechis colletti*	1435.3229^{9+}	12899.8110	n.a.	PLA_2
26	*Pseudechis weigeli*	1039.3342^{7+}		n.a.	3FTx
27	*Crotalus viridis viridis*	1378.8572^{10+}	13769.4645	13769.4670	PLA_2
28	*Crotalus viridis viridis*	1419.0639^{10+}	14203.5345	14189.4790	PLA_2

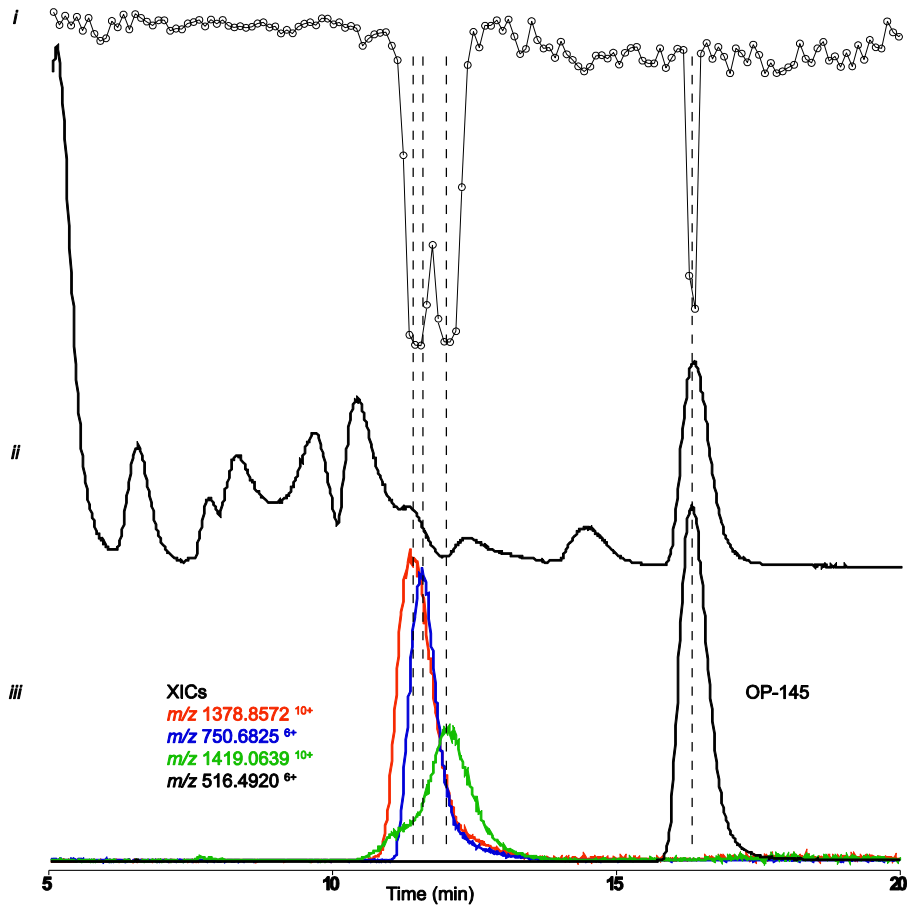

Fig. 4. Screening of prairie rattlesnake venom (*Crotalus viridis viridis*) against *Bacillus subtilis* after at-line nanofractionation. *i* Bioactivity chromatogram represents the results of the resazurin reduction assay for each nanofraction plotted against the time the nanofraction was collected. The peaks with negative maxima represent the bioactive compounds. Fractions were collected with 6-s resolution onto 384-well plates after 50-µL injection of the crude venom at 5 mg/mL concentrations (corresponds to the injection of 250 µg) spiked with OP-145 at 30 µg/mL final concentration (corresponds to injection of 1.5 µg). *ii* The LC−MS chromatogram showing the total ion current (TIC). *iii* The LC−MS data presented as extracted ion currents (XICs) of the *m/z*-values found in the MS spectra corresponding to the bioactive peaks.

most likely that the first peak in the bioactivity chromatogram represents two bioactive proteins with monoisotopic masses 13769.4645 and 4496.0465 Da, while the second bioactive peak has a 14203.5345-Da mass. After the tryptic digestion the molecules found in the bioactive wells were: basic phospholipase A_2 homolog Cax-K49, previously described in *C. atrox* species [Uniprot entry: Q8UVZ7], with the exact monoisotopic mass of 13769.4670 Da for the first bioactive peak, and basic phospholipase A_2 Cvv-N6, previously described in *C. viridis viridis*, with the exact monoisotopic mass of 14189.4790 Da [Uniprot entry: Q71QE8]. These findings do not surprise considering the known antibacterial properties of PLA_2s. The first bioactive protein is most likely the PLA_2 from *C. atrox* found after the tryptic digestion based on the accurate masses measured and identification by MASCOT. The second bioactive could be the PLA_2 from *C. viridis viridis* found after analysis of the tryptic digest, but this has to be confirmed with additional analyses. The difference of approximately 14 Da between the accurate and exact mass could be the consequence of a single amino acid mutation or eventually protein methylation; to the best of our knowledge, this has not been reported before. It is also possible that the bioactive protein is homologous to the PLA_2 from *C. viridis viridis,* sharing part of the sequence identified by the MASCOT search and differing in the rest of the sequence, which results in a different mass. The protein with the mass of 4496.0456 Da could not be identified after tryptic digestion.

The approach described above was applied to analysis of 13 other snake venoms screened after at-line nanofractionation. All bioactive proteins detected are listed in Table 1 together with information on their *m/z* values measured by MS, and their corresponding deconvoluted monoisotopic masses. Next to that, the corresponding theoretical monoisotopic masses of the proteins identified after nanoLC-MS/MS analysis of the tryptic digests, and their toxin family, are listed in Table 1. Many bioactive proteins could not be fully identified via a MASCOT search because of the lack of information in the databases used. However, the MASCOT searches resulted in similar proteins present in species for which appropriate data was available due to shared amino acid sequences. For these partially-identified proteins, only the toxin family is given.

4. Discussion

4.1. Antibacterial activity of crude venoms

We screened 41 crude snake venoms for their antibacterial properties using Bioscreen and the honeycomb plate assay. This assay gave a number of advantages when compared to the traditionally used agar-diffusion assay. Firstly, the Bioscreen and honeycomb plates can be used to simultaneously test 200 samples for the inhibition of bacterial growth. Secondly, the assay is inexpensive, since each well requires only 2 µL of sample and 100 µL of cell suspension in an appropriate medium. Thirdly, pipetting of the cell suspension can be performed rapidly using a multichannel pipettor. Finally, the information obtained gives a better overview of antibacterial activity. In the honeycomb plate the full growth profiles of bacteria are obtained, which means that delays in growth and also different levels of inhibition are detected making it easier to quantify and compare the inhibition caused by samples.

Considering the above-mentioned advantages, using the Bioscreen and honeycomb plates is highly recommended for high-throughput screening of antibacterial activity, especially because the design of these plates in combination with the specific platereader detection cell minimizes the edge effect. Alternatively, O.D. measurements at 600 nm can be used with other microtiter plate formats, including standard 96 or 384-well plates, and appropriate plate readers. However, in these

cases, it would be important to have a humidifying cell installed in the plate reader for O/N measurements in order to reduce evaporation (minimizing the edge effect).

4.2. Antibacterial activity of snake venoms after at-line nanofractionation, detection and identification of antibacterials

At-line nanofractionation was successfully applied to the coupling of LC-MS and the resazurin reduction assay for antibacterial assessment of crude snake venoms, which resulted in detection of compounds with antibacterial activity belonging to the PLA_2 (approximately 13 kDa) and three-finger toxin (3FTx) (approximately 6–8 kDa) families. The detection of compounds was facilitated by high-resolution fractionation (6-s/well), as described previously (Mladic et al., 2016, 2017). Interestingly, higher molecular weight proteins, such as SV-MPs (approximately 25 kDa) and SV-LAAOs (approximately 60 kDa), which are known for their antibacterial activity, were not detected as bioactive using this method. Most likely the low concentration of these proteins in nanofractionated wells was the reason for not detecting them as bioactive. The low concentration of these proteins in nanofractionated well could have been caused by: low concentration of a protein in crude venom, poor solubility of a protein in the assay medium after the evaporation step and/or (partial) denaturation due to the high concentration of ACN in the mobile phase during the reversed phase LC separation. It is also possible that the antibacterial activity of these proteins was inhibited by the activity of bacterial proteases produced by *B. subtilis*, which was used as the test organism for antibacterial activity after nanofractionation. As was expected, many compounds detected belong to the PLA_2 family which is known to possess antibacterial activity. In addition, many 7 kDa compounds were identified as having bioactivity. These compounds belong to the 3FTx family and are known to possess cytotoxic and/or neurotoxic activity. To the best of our knowledge, except for an old study from 1968 (Aloof-Hirsch et al., 1968) which described a 7 kDa direct lytic factor in venom of the rinkhals (*Hemachatus haemachatus*), no studies have reported 3FTxs antibacterial activity. However, it is possible that the primary cytotoxic activity of 3FTxs accounts for the activity of rinkhals venom against bacterial cells, and that this action is therefore not a specific antibacterial action. Certainly, for any compound to be of therapeutic value as an antibacterial, it should have little or no cytotoxic activity against human cells.

We have demonstrated here that at-line nanofractionation has advantages over the traditional BGF approach for fast screening and detection of antibacterial proteins present in complex mixtures such as snake venoms. This supports our previous work (Mladic et al., 2016, 2017) as in many of the venoms analyzed bioactive compounds can be directly assigned to their accurate masses based on retention time and peak shapes detected in both bioactivity and LC-MS chromatograms. In this way, the analysis time is shortened and more information is acquired after only one LC-MS run. This is especially useful to avoid detection/identification of already known bioactive compounds which is common when using the traditional BGF approach. Moreover, identification of bioactive proteins can be performed straightforwardly and without purification. We demonstrated this using nanoLC-MS/MS analysis of tryptic digests of bioactive wells. However, it should be noted that the full identification of unknown proteins may still require purification followed by LC-MS/MS or Edman degradation sequencing, which is also the case when working with species which are not in the search databases.

Author contributions

M.M. conceived, designed and performed the experiments, analyzed the data and wrote the paper; J.S. designed and performed the experiments and analyzed the data; J.K. and F.V. contributed reagents/materials/analysis tools; M.K.R., G.P. vW, and J.K, conceived the project and edited the paper.

Conflicts of interest

The authors declare no conflict of interest. The founding sponsors had no role in the design of the study; in the collection, analyses, or interpretation of data; in the writing of the manuscript, and in the decision to publish the results.

Acknowledgments

This work was supported by by grant nr 731.014.206 from the Netherlands Organization for Scientific Research (NWO) to M.K.R. and G.P.vW.

Appendix A. Supplementary data

Supplementary data related to this article can be found at https://doi.org/10.1016/j.toxicon.2018.08.009.

References

Aloof-Hirsch, S., de Vries, A., Berger, A., 1968. The direct lytic factor of cobra venom: purification and chemical characterization. Biochim. Biophys. Acta 154, 53–60.
Cook, J.J., Bednar, B., Lynch, J.J., Gould, R.J., Egbertson, M.S., Halczenko, W., Duggan, M.E., Hartman, G.D., Lo, M.W., Murphy, G.M., Deckelbaum, L.I., Sax, F.L., Barr, E., 1999. Tirofiban (Aggrastat (R)). Cardiovasc. Drug Rev. 17, 199–224.
de Oliveira Junior, N.G., e Silva Cardoso, M.H., Franco, O.L., 2013. Snake venoms: attractive antimicrobial proteinaceous compounds for therapeutic purposes. Cell. Mol. Life Sci. 70, 4645–4658.
Heus, F., Vonk, F., Otvos, R.A., Bruyneel, B., Smit, A.B., Lingeman, H., Richardson, M., Niessen, W.M.A., Kool, J., 2013. An efficient analytical platform for on-line microfluidic profiling of neuroactive snake venoms towards nicotinic receptor affinity. Toxicon 61, 112–124.
King, G.F., 2011. Venoms as a platform for human drugs: translating toxins into therapeutics. Expet Opin. Biol. Ther. 11, 1469–1484.
McCleary, Ryan J.R., T.S.K.a.R.M.K, 2015. Venoms to Drugs: Venom as a Source for the Development of Human Therapeutics. The Royal Society of Chemistry.
Mladic, M., Zietek, B.M., Iyer, J.K., Hermarij, P., Niessen, W.M., Somsen, G.W., Kini, R.M., Kool, J., 2016. At-line nanofractionation with parallel mass spectrometry and bioactivity assessment for the rapid screening of thrombin and factor Xa inhibitors in snake venoms. Toxicon 110, 79–89.
Mladic, M., de Waal, T., Burggraaff, L., Slagboom, J., Somsen, G.W., Niessen, W.M.A., Manjunatha Kini, R., Kool, J., 2017. Rapid screening and identification of ACE inhibitors in snake venoms using at-line nanofractionation LC-MS. Anal. Bioanal. Chem. 409, 5987–5997.
Munoz, L.J.V.E.-G.,S., 2014. Purification and characterization of venom components as source for antibiotics. Mini-Reviews Org. Chem. 11, 15–27.
Nair, D.G., Fry, B.G., Alewood, P., Kumar, P.P., Kini, R.M., 2007. Antimicrobial activity of omwaprin, a new member of the waprin family of snake venom proteins. Biochem. J. 402, 93–104.
Oguiura, N., Boni-Mitake, M., Affonso, R., Zhang, G., 2011. In vitro antibacterial and hemolytic activities of crotamine, a small basic myotoxin from rattlesnake Crotalus durissus. J. Antibiot. (Tokyo) 64, 327–331.
Okubo, B.M., Silva, O.N., Migliolo, L., Gomes, D.G., Porto, W.F., Batista, C.L., Ramos, C.S., Holanda, H.H.S., Dias, S.C., Franco, O.L., Moreno, S.E., 2012. Evaluation of an antimicrobial L-amino acid oxidase and peptide derivatives from bothropoides mattogrosensis pitviper venom. PLoS One 7.
Otvos, R.A., Heus, F., Vonk, F.J., Halff, J., Bruyneel, B., Paliukhovich, I., Smit, A.B., Niessen, W.M.A., Kool, J., 2013. Analytical workflow for rapid screening and purification of bioactives from venom proteomes. Toxicon 76, 270–281.
Paramo, L., Lomonte, B., Pizarro-Cerda, J., Bengoechea, J.A., Gorvel, J.P., Moreno, E., 1998. Bactericidal activity of Lys49 and Asp49 myotoxic phospholipases A(2) from Bothrops asper snake venom - synthetic Lys49 myotoxin II-(115-129)-peptide identifies its bactericidal region. Eur. J. Biochem. 253, 452–461.
Santamaria, C., Larios, S., Angulo, Y., Pizarro-Cerda, J., Gorvel, J.P., Moreno, E., Lomonte, B., 2005. Antimicrobial activity of myotoxic phospholipases A(2) from crotalid snake venoms and synthetic peptide variants derived from their C-terminal region. Toxicon 45, 807–815.
Scarborough, R.M., 1999. Development of eptifibatide. Am. Heart J. 138, 1093–1104.
Sekiguchi, M., Iida, S., 1967. Mutants of Escherichia coli permeable to actinomycin. Proc. Natl. Acad. Sci. U. S. A. 58, 2315–2320.
Smith, C.G., Vane, J.R., 2003. The discovery of captopril. FASEB J. 17, 788–789.
Torres, A.M., Wong, H.Y., Desai, M., Moochhala, S., Kuchel, P.W., Kini, R.M., 2003. Identification of a novel family of proteins in snake venoms. Purification and structural characterization of nawaprin from Naja nigricollis snake venom. J. Biol. Chem. 278, 40097–40104.
Wang, Y., Hong, J., Liu, X., Yang, H., Liu, R., Wu, J., Wang, A., Lin, D., Lai, R., 2008. Snake cathelicidin from Bungarus fasciatus is a potent peptide antibiotics. PLoS One

3, e3217.
Xie, J.P., Yue, J., Xiong, Y.L., Wang, W.Y., Yu, S.Q., Wang, H.H., 2003. In vitro activities of small peptides from snake venom against clinical isolates of drug-resistant Mycobacterium tuberculosis. Int. J. Antimicrob. Agents 22, 172–174.
Zhao, Z., Ma, Y., Dai, C., Zhao, R., Li, S., Wu, Y., Cao, Z., Li, W., 2009. Imcroporin, a new cationic antimicrobial peptide from the venom of the scorpion Isometrus maculates. Antimicrob. Agents Chemother. 53, 3472–3477.
Zhu, H., Swierstra, J., Wu, C., Girard, G., Choi, Y.H., van Wamel, W., Sandiford, S.K., van Wezel, G.P., 2014. Eliciting antibiotics active against the ESKAPE pathogens in a collection of actinomycetes isolated from mountain soils. Microbiology 160, 1714–1725.